Eur. Phys. J. D **35**, 399–404 (2005)
DOI: 10.1140/epjd/e2005-00194-5

THE EUROPEAN PHYSICAL JOURNAL D

Decomposition of purine nucleobases by very low energy electrons

H. Abdoul-Carime[1], J. Langer[1,a], M.A. Huels[2], and E. Illenberger[1]

[1] Institut für Physikalische und Theoretische Chemie, Freie Universität Berlin, Takustrasse 3, 14195 Berlin, Germany
[2] Départment de Médicine et Radiobiologie, Faculté de Médicine, Université de Sherbrooke, Sherbrooke, QC, Canada

Received 31 March 2005
Published online 26 July 2005 –

Abstract. We show that low energy electrons effectively decompose the gas phase purine nucleobases adenine (A) and guanine (G) via dissociative electron attachment (DEA) involving low lying (<3 eV) shape resonances, but also via core excited resonances (located near 6 eV). In adenine the low energy resonances exclusively lead to dehydrogenation, i.e. ejection of a neutral hydrogen radical with the excess electron remaining on the molecule. This reaction by far dominates DEA in the entire energy range 0–15 eV, similar to the situation recently observed in the pyrimidine bases thymine (T), cytosine (C) and uracil (U). In striking contrast to that, guanine behaves very different in that dehydrogenation is comparatively weak while various further decomposition reactions are observed from the low energy π^* precursor ions. These reactions lead to fragment ions of the form $(G–O/NH_2)^-$, O^-/NH_2^-, $(G–HOCN)^-$, OCN^-, CN^- indicative of single bond cleavages but also more complex unimolecular decompositions associated with the excision of cyano units from the cyclic structure. Since electrons are the predominant secondary species in the interaction of high energy quanta with biological material, electron driven reactions represent initial steps in the molecular description of radiation damage.

PACS. 34.80.Ht Dissociation and dissociative attachment by electron impact – 82.30.Lp Decomposition reactions (pyrolysis, dissociation, and fragmentation) – 87.50.Gi Ionizing radiations (ultraviolet, X-rays, gamma-rays, ions, electrons, positrons, neutrons, and mesons, etc.)

1 Introduction

Within the last two decades, reactions driven by low energy electrons have attracted considerable interest in different fields of fundamental and applied science, such as planetary science [1,2], lithography [3,4], tunnelling microscopy [5], and life science [6,7]. For the latter and more particularly in field of radiation biology, the ability of electrons to induce lethal damage to the chromosomes (i.e., nucleic acids or proteins) has been explored only very recently [8–10]. Further extensive experimental [11,12] and theoretical [13–15] investigations have been undertaken to unravel the underlying molecular mechanisms.

The deposition of high energy quanta within cells generates primarily (excited) neutral and charged species, and secondary particles with electrons (<20 eV) as the most predominant ones [7,16,17]. These ballistic electrons may subsequently react with the neighbouring compounds (e.g., water, lipids, proteins, nucleic acids). In this context the action of radicals is subject of numerous investigations [18–20]. On the contrary, the specific action of ballistic secondary electrons is not easy to investigate via the traditional techniques (e.g. pulse radiolysis), since they are formed and remain present in the medium only during a very short time period (fs to ps) [21,22]. Recently, the combination of surface science methodology with biochemical analysis (electrophoresis) provides an adapted tool to investigate experimentally the role of low energy (<30 eV) electrons on DNA to generate strand breaks [8,9,23] via the decomposition of their building-blocks: the sugar backbone and nucleobases (NBs) [24].

The purines adenine and guanine, combined with the pyrimidines thymine (or uracil) and cytosine, represent the four canonical nucleobases for the building of DNA (or RNA). Their individual sequence encodes the genetic information [25] which is required for cell reproduction and for the synthesis of many proteins. Their alteration may lead to dramatic consequences, such as the appearance of chromosomal anomalies in terms of cancers or mutations [26,27]. While the decomposition of the pyrimidine nucleobases by low energy electrons has already been the subject of several investigations [10,28–31], that of the purines have been reported so far essentially from electron stimulated desorption (ESD) experiments [30]. In the ESD technique, the corresponding molecular film is bombarded by a beam of electrons at a defined energy and the desorbed ions are detected mass-spectrometrically. Only ions

[a] e-mail: langerj@chemie.fu-berlin.de

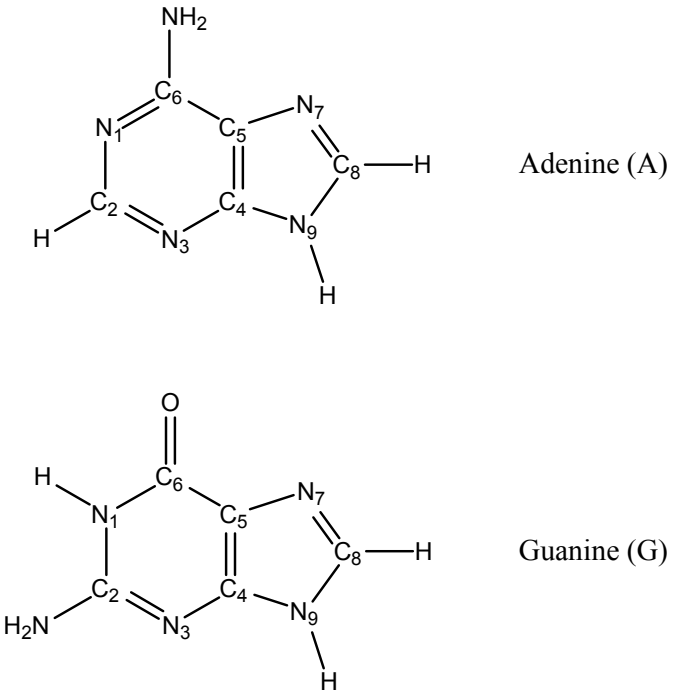

Fig. 1. Structure of adenine (A) and guanine (G) with IUPAC numbered atoms.

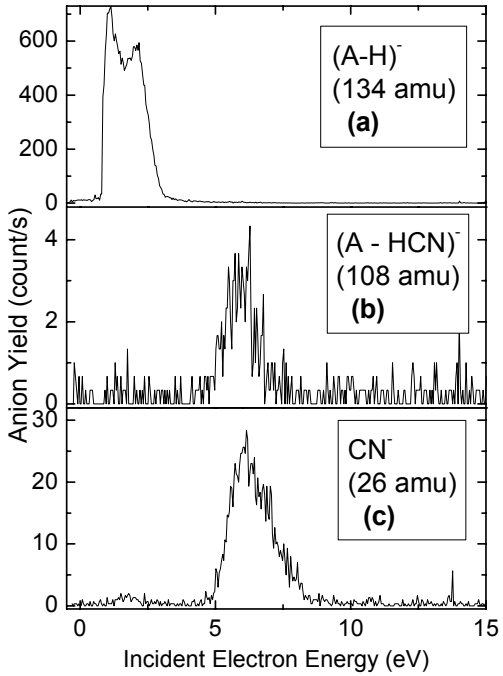

Fig. 2. Ion yield of (a) $(A–H)^-$ (134 amu), (b) $(A–CN)^-$ (109 amu) and (c) CN^- (26 amu) produced from electron impact on gaseous adenine.

that possess sufficient kinetic energy to overcome the attractive forces induced by the environment can leave the surface and may hence be detected [32]. Therefore, such kind of experiments strongly focuses on desorption of light fragment ions. On the contrary, in the complementary gas phase experiments, any negative fragments existing on the mass-spectrometric time scale can be detected.

In the present work, we investigate the intrinsic interaction of low energy electrons with gas phase adenine and guanine whose structures are illustrated in Figure 1. We show that fragmentation of adenine is restricted to a few negatively charged species. In contrast to that, guanine decomposes into a variety of negatively charged species via rather complex unimolecular reaction. Comparative data from adenine and guanine suggest that the latter is less sensitive to electron attacks.

2 Experimental

The experiments were carried out in a standard crossed beam apparatus that has already been described elsewhere [33]. Only the essential features of the experiment are reported in this section. An incident electron beam of well-defined energy (FWHM $\approx$ 150 meV, $I(e^-) \approx$ 10 nA), generated by a trochoidal electron monochromator, crosses orthogonally an effusive molecular beam of adenine or guanine. The beam emanates from an oven containing approximately 50 mg of 99% purity powder (Aldrich Ltd.) heated by two in vacuo halogen bulbs. These lamps also prevent the powder from condensation on the surfaces (plates, chamber walls), which otherwise may lead to undesirable changes in contact potentials during measurements. The operating temperature of approximately 470 K (adenine) and 500 K (guanine) measured by a platinum resistance directly at the oven is below the molecular decomposition temperature (>610 K for guanine [34]). Therefore, the original structure of adenine and guanine produced in the gas phase is likely to remain intact (see also section Discussion). The negative ions formed via electron-molecule collisions are extracted from the reaction volume by a small electric field (<1.0 Vcm^{-1}) towards a quadrupole mass analyzer, and are detected by single pulse counting techniques. The magnitude of a particular anion yield as a function of the incident electron energy (assigned as the ion yield function) is then recorded. The electron energy scale is calibrated by measuring the SF_6^- signal originating from an intense narrow resonance near 0 eV [33]. However, calibration is established before and after taking the ion yield of interest. Indeed, it has been shown that the produced SF_6^- anion can subsequently induce dissociative electron transfer reaction with the investigated substance, generating additional anion signals near 0 eV [35,36].

3 Results

In Figures 2 and 3, we present the ion yields obtained from low energy (<16 eV) electron interaction with adenine and guanine. Both compounds show a resonant feature below 3 eV and a further resonant contribution around 6 eV. We note that in any of the pyrimidine bases, the low energy feature was *exclusively* due to the dehydrogenation

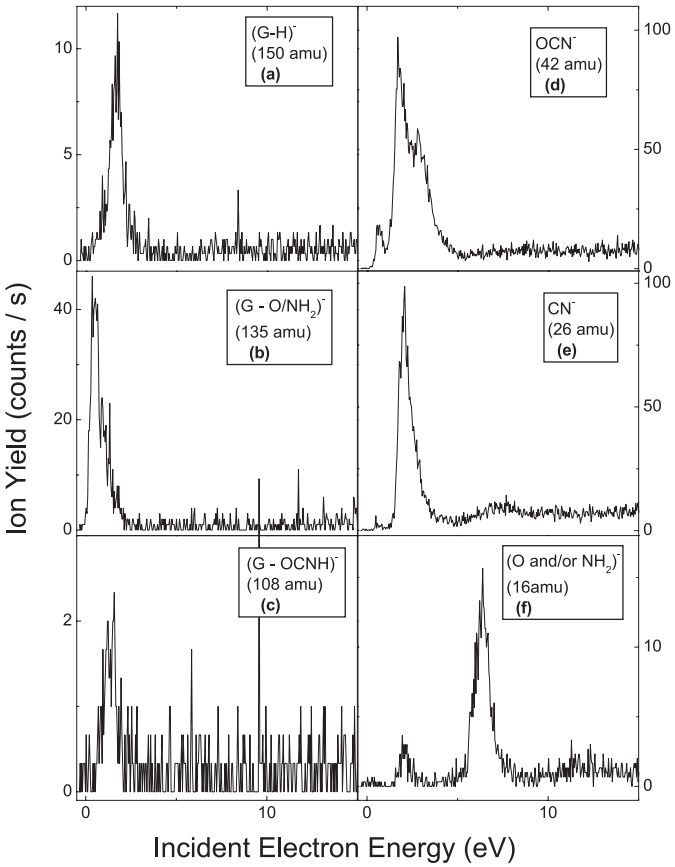

Fig. 3. Ion yield of (a) $(G–H)^-$ (150 amu), (b) $(G–O/NH_2)^-$ (135 amu), (c) $(G–OCNH)^-$ (108 amu), (d) OCN^- (42 amu), CN^- (26 amu) and (f) $(O/NH_2)^-$ (16 amu) anion produced from electron impact on gaseous guanine. In (f) the signal at 2 eV is due to $(NH_2)^-$ (see the text).

reaction, i.e., formation of $(NB–H)^-$ and the associated neutral H radical [10,28]. From Figures 2 and 3, it can be seen that the loss of hydrogen represents the predominant reaction channel in adenine, while guanine decomposes into a whole string of fragments already at low energies.

Fragmentation of adenine produces three main negative fragments attributed to $(A–H)^-$ (134 amu), $(A–HCN)^-$ (108 amu) and CN^- (26 amu), shown in Figure 2. In contrast, the decomposition of guanine by electrons generates more different anionic fragments attributed to $(G–H)^-$ (150 amu), $(G–NH_2)^-$ (135 amu), (see below), $(G–OCNH)^-$ (108 amu), OCN^- (42 amu), CN^- (26 amu) and $(O \text{ and/or } NH_2)^-$ (16 amu), shown in Figure 3. Finally, it is worth mentioning that the evaporation technique produces NBs in different tautomers (e.g., the enol and the keto forms of guanine) [37–39], which are present in the interaction zone.

4 Discussion

The resonant features of the anion yields in Figures 2 and 3 indicate that the underlying process is DEA, which represents the only efficient decomposition mechanism below the ionization energy (8.25 eV for adenine and 8.57 eV for guanine [40]). Here the incoming electron is captured by the nucleobase NB to form a transitory negative ion, $NB^{-\#}$, which can subsequently decompose into a stable negative fragment and one or more neutral counterpart(s). Alternatively, the excess electron can be ejected from $NB^{-\#}$ eventually leaving the molecule in an excited state (auto-detachment).

4.1 Decomposition mechanisms

At energies below the first electronically excited state of adenine and guanine (4.9 eV) [41], the formation of $NB^{-\#}$ must involve a one-particle shape resonance. In that case, the excess charge occupies one of the normally unfilled molecular orbitals. Electron transmission (ET) experiments coupled with ab-initio calculations assign a series of π^* anions in the energy range between 0.5 and 2.5 eV for A, G and their tautomers [39]. We will not try to correlate the ET features with structures observed in our ion yields but instead we note that while ET reflects the initial Frank-Condon transition, in DEA the energy dependent decomposition probability (including auto-detachment [42]) can considerably shift the resonance maximum. Apart from that we can assign the following fragment ions to arise from shape resonances; from adenine: $(A–H)^-$ (1.1 eV and 2.1 eV) and CN^- (1.8 eV), from guanine: $(G–H)^-$ (0.9 eV and 1.7 eV), $(G–O/\ NH_2)^-$ (0.5 eV and 1.4 eV), $(G–OCNH)^-$ (1.3 eV), OCN^- (0.6 eV, 1.7 eV and 2.9 eV), CN^- (2.0 eV) and O^- and/or $NH_2{}^-$ (2.0 eV).

The yield function of $(A–H)^-$ shows a comparatively sharp peak at 1.1 eV. A similar structure at 1.0 eV has also been reported for $(T–H)^-$ and $(U–H)^-$ but not for $(C–H)^-$ [10,28]. In a recent work, it has been postulated that this 1.0 eV peculiar feature appearing in the yield function of $(U–H)^-$ [10,28] arises from the formation of a dipole bound (DB) anion in a vibrationally excited state (DB Feshbach resonance associated to the $\nu = 3$ level of the N1–H stretch vibration) which couples to the $\sigma_{N1-H}{}^*$ state [31]. A dipole bound anion consists of the binding of the excess electron into a diffuse orbital outside the molecular frame by multipole moments and the polarizability [43,44]. The critical dipole moment of a molecule to form DB anions requires values from 2 to 2.5 D. The dipole moments of the nucleobases are 2.5 D (A), 4.2 D (T), and ≈7 D (C; G) [44]. DB nucleobase anions have been predicted [45,46] and observed experimentally in supersonic expansion, where the nucleobases are cooled down to 100 K [47,48]. There are, however, no obvious reasons why dehydrogenation of thymine, uracil and adenine proceeds via the formation of a dipole bound state, and why this is not the case for cytosine and guanine. We finally note that vibrationally excited DB anions undergo fast auto-detachment [49], which may rise questions concerning the interpretation of the sharp structure at 1.1 eV (in thymine and uracil) [10,28].

Negative ions formed from the higher electron feature closed to 6 eV can be assigned as core excited resonances.

In that case, the incoming electron induces an electronic transition (e.g., $\pi \rightarrow \pi^*$), being simultaneously captured by the field of the positive core [50–52]. Thus, $(A–HCN)^-$ (5.8 eV), CN^- (6.0 eV and 7.5 eV) detected from adenine, and CN^- (7.5 eV) and O^- and/or NH_2^- (6.2 eV) from guanine are likely to arise from core excited resonances. In particular, the resonance located at 5.8 eV for $(A–HCN)^-$ and CN^- (6.0 eV) in adenine (Fig. 2) may be associated to the excitation of the $4^1A'(^1B_b)$ state, and those resonance at 7.5 eV to the $7^1A'$ state. The O^- and/or NH_2^- resonance in guanine around 6.2 eV may be attributed to the $5^1A'$ state [52].

Figure 3 shows that below 3 eV, $G^{-\#}$ decays into 6 different channels. As mentioned above, the transient negative ion is characterized by shape resonances associated to the keto or enol form of the nucleobase [39]. These π^* states decompose either by single bond cleavage ($(G–H)^-$, $(G–NH_2)^-$ and O^- and/or NH_2^-) or more complex reactions associated with the excision of the cyano and isocyano groups from the six-membered ring or the imidazole ring system ($(G\text{-}HOCN)^-$, OCN^- and CN^-).

From the present observation of fragment anions arising from the degradation of the cyclic structure in G already at very low electron energies, one might be tempted to assume that the molecule is subjected to thermal decomposition during the sublimation procedure. From the presence of the $(G–H)^-$ signal, however, we can conclude that intact guanine molecules are present in the reaction zone. Furthermore, thermal decomposition of G was explicitly followed in a photoelectron (PE) study of gaseous guanine [34]. Decomposition of G was found (via degradation of bands in the PE spectrum) for temperatures above 610 K and when heating the sample for longer than 30 minutes. Since we performed sublimation at a considerably lower temperature (500 K), we conclude that G is thermally not decomposed.

4.2 Energetics

In the following, the energetics for the decomposition of the $NB^{-\#}$ will be discussed. The thermodynamic threshold ΔH_0 for a simple bond dissociation process in a molecule RX initiated by electron interaction, $e^- + RX \rightarrow R + X^-$, can be expressed as:

$$\Delta H_0(X^-) = D(R - X) - EA(X) \qquad (1)$$

ΔH_0 (X^-) is the threshold energy for the observation of X^-, D(R–X) the bond dissociation energy and EA(X), the electron affinity of the corresponding radical.

Dehydrogenation of adenine and guanine arises from the cleavage of either the C–H or one of the N–H bonds (the ring N–Hs or amino N–H, see Fig. 1). Ab-initio calculations in adenine predict the bond dissociation energies for the different positions [53] ranging from 4.33 to 5.03 eV and the electron affinities of the corresponding radicals [54] ranging from 0.97 to 3.23 eV. Based on these values, the thermodynamic threshold spans from 1.1 eV (N9–H) to 3.7eV (C2–H). Therefore, we suggest that at the experimental threshold (0.7 eV) the N9–H bond is cleaved. The small energy difference can be accounted to excitation of the hot molecule. From the binding energy D(N–H) = 3.95 eV [55] and the electron affinity EA(G–H) = 3.46 eV [55], we can estimate the threshold for the dehydrogenation of guanine to be $\Delta H_0 = 0.49$ eV, which is in a good agreement with the experimental result (0.5 eV).

The 135 amu negative fragment produced from guanine can a priori be attributed to either $(G–O)^-$ or $(G–NH_2)^-$. The formation of the former fragment would require substantial energy due to large value of the C–O double bond (≈7.5 eV [56]). Therefore, we conclude that $(G–NH_2)^-$ is rather formed than $(G–O)^-$. In this case, the electron affinity of the $(G–NH_2)$ radical must exceed the value of $D(C–NH_2) = 3.9$ eV [56] to drive such a reaction already at the appearance energy close to 0 eV.

The 16 amu fragment can a priori be attributed to O^- or NH_2^-. According to the known electron affinities of O (1.46 eV) and NH_2 (0.77 eV) [57], and the dissociation energies $D(C{=}O) = 7.5$ eV and $D(C–NH_2) = 3.9$ eV [56], the estimated thresholds are 6.1 eV and 3.1 eV, respectively. Since the experimental threshold of the 16 amu anion is close to 1.5 eV, we conclude that only NH_2^- is formed at such low energies. The appreciably lower experimental appearance energy with respect to the calculated one (1.6 eV) can be attributed to thermal excitation of the molecule with its 42 vibrational degrees of freedom (apart from possible uncertainties in the above values for the determination of the threshold). This is strongly supported by the fact that the low energy feature is much weaker than that near 6 eV indicating that only a minority of highly excited species can access the dissociation channel. In DEA the general cross-section behavior is *reciprocal* with energy leading to much stronger signals towards lower electron energies. On the other hand, from the core excited resonance at 6 eV both O^- and NH_2^- can be formed.

The formation of OCN^- and CN^- in guanine and CN^- in adenine requires more complex dissociation pathways driven by the high electron affinity of OCN (3.61 eV) and CN (3.82 eV) [57]. The formation of these fragments must be accompanied by a substantial rearrangement of the molecular rings. We here resist from further speculations on the structure of possible neutral counterparts to these negatively charged species. Very recent ab-initio calculations predict a serious buckling of the molecular skeleton following electron attachment to guanine [38] which may be the origin of the degradation of the cyclic structure. The distortion of the geometry on going from the neutral to the anion is particularly pronounced in the guanine molecule.

Finally, it is noteworthy that guanine loses an isocyanic acid, OCNH, at low energy (1.3 eV), while a cyanic acid, HCN is cleaved from adenine, at higher energy (5.8 eV).

4.3 Cross-sections

A reference for the decomposition efficiency of a nucleobase into a specific DEA channel is the partial DEA

cross-section. In a simplified scheme, we use the signal intensity of our calibration substance $S_{SF_6^-}$, and the well-known cross-section for thermal electron attachment to SF_6^- ($\sigma_{SF_6^-} \approx 4 \times 10^{-14}$ cm^2 [58]) to estimate the DEA cross-section for a certain product anion. This is a very rough approximation (expected accuracy order of magnitude) since the energy resolution presently used is appreciably larger than the width of a thermal distribution, on which the SF_6^- cross-section is based. Within the assumption, that the proportionality factor for detecting the calibration compound SF_6^- is sufficiently similar to the negative anion under consideration, and the measured anion signal, S_{anion}, is linearly proportional to the number density of the target, ρ_g, σ_{anion} can be given as follows [33]:

$$\frac{\sigma_{anion}}{\sigma_{SF_6^-}} \approx \frac{S_{anion}}{S_{SF_6^-}} \frac{\rho_{SF_6^-}}{\rho_g}. \quad (2)$$

We then calculate the DEA cross-section of $(G–NH_2)^-$ formed to be 2×10^{-17} cm^2. The DEA cross-section of $(A–H)^-$ (1.1 eV) and $(G–H)^-$ (1.7 eV) results to be 9×10^{-16} cm^2 and 5×10^{-18} cm^2, respectively. These values are comparable with the estimated DEA cross-sections for $(T–H)^-$, $(U–H)^-$ and $(C–H)^-$ at 1.0 eV (1×10^{-15} cm^2, 3×10^{-16} cm^2 and 2×10^{-16} cm^2, respectively [10,28]).

In any of these nucleobases, the dehydrogenation reaction is by far the dominant channel in electron attachment, within the 0–16 eV energy range. However, the remarkable exception is guanine for which this reaction is about one order of magnitude weaker than for the other nucleobases. Figure 2 demonstrates that in adenine the dehydrogenation channel represents about 95% of the total yield. In striking contrast, in guanine, the dehydrogenation reaction represents only about 5% of the total yield (Fig. 3).

Interestingly, even at sub-excitation energies, G decomposes into a variety of DEA channels. If we calculate the total DEA cross-section in guanine (integrating over the total ion yield within the 0–15 eV energy range) we arrive at a value of 10^{-15} cm^2, which is still smaller than all the other nucleobases. For instance, the averaged total decomposition cross-section (0–16 eV) of adenine is by the factor 2.2 higher than that of guanine. These findings suggest that guanine is the less sensitive nucleobase to the electron attack.

5 Conclusion

From the present results it can be seen that out of the isolated nucleobases (U, T, A, G and C), guanine (G) behaves particular in the way that (i) the cross-section for DEA is appreciably lower and (ii) the anionic precursors formed at sub-excitation energy decompose into a variety of fragment ions also associated with the degradation of the cyclic structure. While the other nucleobases (U, T, A, and C) also do form transient anions at low energy, these anions exclusively abstract a neutral hydrogen from the N positions. For a nucleobase coupled in the DNA network this means that in the case of U, T, A, and C the base can act as acceptor of low energy electrons which are eventually transferred (via the N–C bond) to the backbone inducing strand breaks. Such a scenario was recently proposed in a theoretical study by Berdys et al. [15] by modeling a section of DNA containing a cytosine base, the sugar ring and the (neutralized) phosphate group. They find a low lying anionic curve connecting the initial π^* anion state of the base to a σ^* state in the backbone leading to rupture of the C–O bond between the sugar and the phosphate. Our findings show that in G the cross-section for accepting sub-excitation electrons is lower and once the anion is formed it decomposes, and consequently the above scenario of excess charge transfer can probably not operate. Of course, the variety of radicals produced at sub-excitation energy can induce complex chemistry eventually also leading to strand breaks.

This work is supported by the European Union, the German Science Foundation (DFG) Freie Universität Berlin. HAC is a fellow of the European Union EPIC (Electron and Positron Induced Chemistry) EU-Network.

References

1. T.M. Orlando, M.T. Sieger, W.C. Simpson, Nature **394**, 554 (1998)
2. Q.-B. Lu, T.E. Madey, Phys. Rev. Lett. **82**, 4122 (1999)
3. K. Wilder, C.F. Qate, B. Singh, D.F. Kyser, J. Vac. Sci. Tech. B **16**, 3864 (1998)
4. A. Golhauser, W. Meyer, V. Stadler, W. Eck, M. Grunze, K. Edinger, Th. Weimann, P. Hinze, J. Vac. Technol. B **18**, 3414 (2000)
5. J.I. Pascual, N. Lorente, Z. Song, H. Conrad, H.-P. Rust, Nature **423**, 525 (2003)
6. D.W. Gidley, A. Rich, J. Van House, P.W. Zitzewitz, Nature **297**, 639 (1982)
7. M. Inokuti, In *Radiation Physics as a Basis of Radiation Chemistry and Biology*, Applied Atomic Collision Physics (Academic Press Inc., 1983), Vol. 4, p. 179
8. B. Boudaïffa, P. Cloutier, D. Hunting, M.A. Huels, L. Sanche, Science **287**, 1658 (2000)
9. F. Martin, P.D. Burrow, Z. Cai, P. Cloutier, D. Hunting, L. Sanche, Phys. Rev. Lett. **93**, 681011 (2004)
10. H. Abdoul-Carime, S. Gohlke, E. Illenberger, J. Am. Chem. Soc. **126**, 12158 (2004)
11. L. Sanche, Mass. Spectrom. Rev. **21**, 349 (2002)
12. R. Balog, J. Langer, S. Gohlke, M. Stano, H. Abdoul-Carime, E. Illenberger, Int. J. Mass Spectrom. **233**, 267 (2004)
13. X. Li, M.D. Sevilla, L. Sanche, J. Phys. Chem. B **108**, 19013 (2004)
14. F.A. Gianturco, R.R. Lucchese, J. Chem. Phys. **120**, 7446 (2004)
15. J. Berdys, I. Anusiewicz, P. Skurski, J. Simons, J. Am. Chem. Soc. **126**, 6441 (2004)
16. *Charged Particle and Photon Interactions with Matter*, edited by A. Mozumder, Y. Hatano (Marcel Dekker, New York, 2004)
17. 10^4 electrons are created per 1 MeV deposited; ICRU Report 31, International Commission on Radiation Units and Measurements, Washington DC (1979)

18. C.V. von Sonntag, The Chemical Basis of Radiation Biology (Taylor & Francis, London, 1987)
19. *Radiation Damage in DNA: Structure/Function Relationships at Early Times*, edited by A.F. Fuciarelli, J.D. Zimbrick (Batelle, Columbus, OH, 1995)
20. M.J. Davis, R.T. Jones, In *Radical Mediated Protein Oxidation: from Chemistry to Medicine* (Oxford University Press, Oxford, 1997)
21. S.M. Pimblott, J.A. La Verne, A. Mozumder, N.J.B. Green, J. Phys. Chem. **94** 488 (1990)
22. V. Cobut, Y. Fongillo, J.P. Patau, T. Goulet, M.-J. Fraser, J.-P. Jay-Gerin, Radiat. Phys. Chem. **51**, 229 (1998)
23. X. Pan, P. Cloutier, D. Hunting, L. Sanche, Phys. Rev. Lett. **90**, 2081021 (2003)
24. H. Abdoul-Carime, P.C. Dugal, L. Sanche, Radiat. Res. **153**, 23 (2000)
25. J.D. Watson, F.H.C. Crick, Nature **171**, 737 (1953)
26. H.J. Helbock, K.B. Beckman, M.K. Shigenaga, P.B. Walter, A.A. Woodall, H.C. Yeo, B.N. Ames, PNAS USA **95**, 288 (1998)
27. E. Cavalieri, K. Frenkel, J.G. Liehr, E. Rogan, D. Ray, J. Natl. Cancer Inst. Monogr. **27**, 75 (2000)
28. G. Hanel, B. Gstir, P. Scheier, M. Probst, B. Farizon, M. Farizon, E. Illenberger, T.D. Märk, Phys. Rev. Lett. **90**, 1881041 (2003)
29. M.-A. Hervé du Penhoat, M.A. Huels, P. Cloutier, J.-P. Jay-Gerin, L. Sanche, J. Chem. Phys. **114**, 5755 (2001)
30. H. Abdoul-Carime, P. Cloutier, L. Sanche, Radiat. Res. **155**, 625 (2001)
31. A.M. Scheer, K. Aflatooni, G.A. Gallup, P.D. Burrow, Phys. Rev. Lett. **92**, 681021 (2004)
32. H. Sambe, D.E. Ramaker, L. Parenteau. L. Sanche, Phys. Rev. Lett. **59**, 236 (1987)
33. E. Illenberger, *Gaseous Molecular Ions* (Steinkopff, Springer, Darmstadt, New York, 1992), Vol. 2
34. J. Lin, C. Yu, S. Peng, I., Akiyama, K. Li, L. Kao Lee, P.R. LeBreton, J. Phys. Chem. **84**, 1006 (1980)
35. S. Gohlke, H. Abdoul-Carime, E. Illenberger, Chem. Phys. Lett. **380**, 595 (2003)
36. H. Abdoul-Carime, S. Gohlke, E. Illenberger, Chem. Phys. Lett. **402**, 497 (2005)
37. M. Mons, I. Dimicoli, F. Piuzzi, B. Tardivel, M. Elhanine, J. Phys. Chem. A **106**, 5088 (2002)
38. M. Haranczyk, M. Gutkowsky, J. Am. Chem. Soc. **127**, 699 (2005)
39. K. Aflatooni, G.A. Gallup, P.D. Burrow, J. Phys. Chem. A **102**, 6205 (1998)
40. A.-O. Colson, B. Besler, D.M. Close, M.D. Sevilla, J. Phys. Chem. **96**, 661 (1992)
41. A.V. Crewe, M. Isaacson, D. Johnson, Nature **231**, 262 (1971)
42. T.F. O'Malley, Phys. Rev. **150**, 14 (1966)
43. E. Fermi, E. Teller, Phys. Rev. **72**, 399 (1947)
44. H. Abdoul-Carime, C. Defrançois, Eur. Phys. J. D **2**, 149 (1998)
45. D.M. Smith, A.F. Jalbout, J. Smets, L. Adamowicz, Chem. Phys. **260**, 45 (2000)
46. E.C.M. Chen, E.S. Chen. J. Phys. Chem. B **104**, 7835 (2000)
47. C. Desfrançois, H. Abdoul-Carime, J.-P. Schermann, J. Chem. Phys. **104**, 7792 (1996)
48. C. Desfrançois, H. Abdoul-Carime, C.P. Schulz, J.-P. Schermann, Science **269**, 1707 (1995)
49. B. Lucas, F. Lecomte, B. Reiman, H.D. Barth, G. Gregoire, Y. Bouteiller, J.P. Schermann, C. Desfrançois, Phys. Chem. Chem. Phys. **6**, 2600 (2004)
50. B. Mely, A. Pullman, Theoret. Chim. Acta **13**, 278 (1969)
51. P.R. Callis, Ann. Rev. Phys. Chem. **34**, 329 (1983)
52. M.P. Fülscher, L. Serrano-Andrès, B.O. Roos, J. Am. Chem. Soc. **119**, 6188 (1997)
53. M. Zierhut, W. Roth, I. Fischer, Phys. Chem. Chem. Phys. **6**, 5178 (2004)
54. F.A. Evangelista, A. Paul, H.F. Schaeffer III, J. Phys. Chem. A **108**, 3565 (2004)
55. E.S.D. Chen, E.C.M. Chen, N. Sane, Biochem. Biophys. Res. Comm. **246**, 228 (1998)
56. T.H. Lowry, K.S. Richardson, *Mechanism and Theory in Organic Chemistry*, 3rd edn. (Harper Collins Publishers, 1987)
57. J.C. Rienstra-Kiracofe, G.S. Tschumper, H.F. Schaeffer III, S. Nandi, G.B. Ellison. Chem. Rev. **102**, 231 (2002)
58. D. Smith, N.G. Adams, E. Alge, J. Phys. B: At. Mol. Phys. **17**, 461 (1984)